NANO LETTERS

2008
Vol. 8, No. 5
1291-1295

Conductance of Oriented C_{60} Molecules

Nicolas Néel, Jörg Kröger,* Laurent Limot,† and Richard Berndt

Institut für Experimentelle und Angewandte Physik, Christian-Albrechts-Universität zu Kiel, D-24098 Kiel, Germany

Received November 25, 2007; Revised Manuscript Received January 28, 2008

ABSTRACT

C_{60} molecules adsorbed to Cu(100) are contacted with the tip of a cryogenic scanning tunneling microscope. Images with submolecular resolution reveal distinct orientations of the molecules. We find that the orientation significantly affects the conductance of the contact despite the high symmetry of C_{60}.

Molecules employed as active device components within molecular electronic circuits could offer interesting technological opportunities.[1–5] The electronic, optical, and magnetic properties of a molecule can be tuned through chemical composition and structure to perform the desired task at the molecular level. A key challenge in molecular electronics is to translate the solution or gas-phase design into a solid-state device. Advances in the manipulation of single objects now permit one to contact atoms and molecules between two electrodes,[6–13] and measure electron transport through conductance histograms,[14–17] although the details of the molecular junction are usually not directly known. The emerging picture, based on theoretical work[18–21] as well as on experiments on metallic single atom contacts,[21,22] however, indicates that details of the interface can significantly alter the conductance. An increased control over the molecular orientation and the electrode status is therefore most desirable.

To investigate the important role of the contact geometry, we have studied the prototypical molecular contact of a single C_{60} molecule attached to copper contacts in different orientations using a low-temperature scanning tunneling microscope. C_{60} molecules on a Cu(100) single crystal surface are particularly suitable as a model system because the tip−molecule contact is sufficiently stable to withstand currents of the order of 10 μA through a molecule without damage to tip or sample.[12] At low temperatures, the molecule under investigation and its environment can be imaged prior to and after contact and molecular orientations can be distinguished because no thermally excited molecular rotation occurs. Moreover, the status of the microscope tip, which serves as a second electrode, can be monitored to some extent from concomitant measurements on adjacent pristine surface areas. Consequently, as the tip is approached closer to a molecule, a reproducible variation of the conductance is observed. This variation is typical of all molecules in a specific bonding geometry at the surface. In the present study, we find a remarkable influence of the contact geometry on the molecular conductance.

Experiments were performed using a scanning tunneling microscope operated at 8 K and in ultrahigh vacuum with a base pressure of 10^{-9} Pa. Cu(100) surfaces as well as chemically etched tungsten tips were prepared by argon ion bombardment and annealing. C_{60} molecules of 99.99% purity were sublimed from a tantalum crucible with the sample surface at room temperature. An ordered fullerene film was obtained by annealing the surface after deposition at 500 K for several minutes. An adsorbate-induced missing-row reconstruction of the copper surface leads to molecules residing in single and double missing rows.[23] Scanning tunneling microscopy (STM) images were acquired in constant-current mode with the voltage applied to the sample. Spectroscopy in the tunneling as well as in the contact regime was performed by superimposing a sinusoidal voltage signal (1 mV root-mean-square, 8 kHz) on the tunneling voltage and measuring the current response by a lock-in amplifier.

Upon adsorption on Cu(100), C_{60} adopts five orientations as revealed by the submolecular patterns detected in vacuum (Figure 1a). These orientations are directly linked to the bonding geometry with the substrate. The four orientations relevant to this work are encircled by dashed lines in Figure 1a and shown as close-up views in Figure 1b. We analyzed the submolecular structure using the spatial distribution of the second-to-lowest unoccupied molecular orbital (LUMO + 1).[24,25] C_{60} in single missing rows exposes a C−C bond between either a carbon pentagon and hexagon (**1** in Figure 1) or two carbon hexagons (**2**), molecules located in double missing rows expose either a carbon pentagon at the top (**3**) or a carbon hexagon (**4**).

* Corresponding author. E-mail: kroeger@physik.uni-kiel.de. Telephone: +49 431 8803966. Fax: +49 431 8801685.

† Laurent Limot, Institut de Physique et Chimie des Matériaux de Strasbourg, Université Louis Pasteur, F-67034 Strasbourg, France.

10.1021/nl073074i CCC: $40.75
Published on Web 04/03/2008

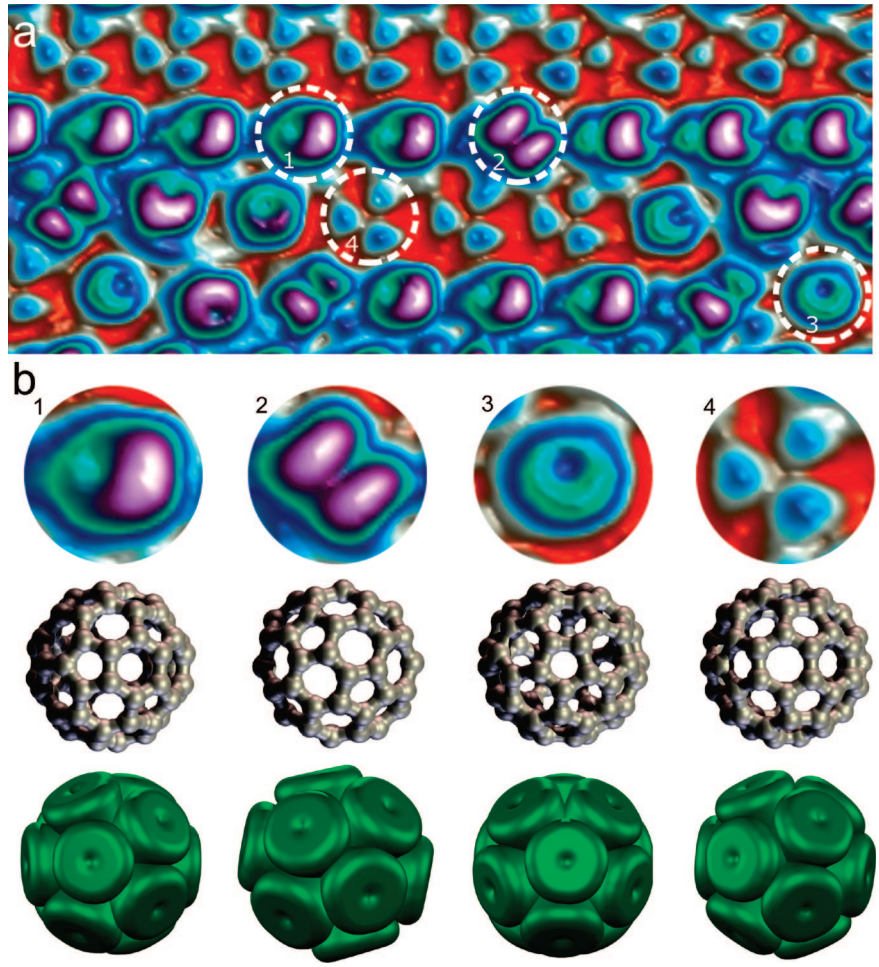

Figure 1. (a) Quasi-three-dimensional STM image of a C_{60} island on Cu(100) (sample voltage $V = 1.5$ V, current $I = 1$ nA, size 85 Å × 35 Å). Molecule orientations **1**−**4** are indicated by dashed circles. (b) Close-up view of C_{60} molecules (top row) arranged according to their submolecular patterns exposed to vacuum. **1**: hexagon:pentagon bond; **2**: hexagon:hexagon bond; **3**: pentagon; **4**: hexagon. Middle and bottom row show models of C_{60} and spatial distributions of the second-to-lowest unoccupied molecular orbital for the respective orientations **1**−**4**.

Having identified the orientations of interest, a tip−molecule contact was then achieved by centering the tip above a single C_{60} and subsequently approaching it vertically at a speed of 45 Å s^{-1}. We observed that small lateral offsets of the tip position did not drastically change the results. The overall shape of the conductance curve for orientation **1** with tip displacement is shown in Figure 2a. The conductance is defined as $G = I/V$ (I: current, V: sample voltage) in units of the quantum of conductance $G_0 = 2e^2/h$ ($-e$: electron charge, h: Planck's constant). The conductance curve has already been discussed in ref 12. Below, we summarize the relevant characteristics. In the tunneling regime (denoted I in Figure 2a), at small tip displacements Δz between 0 to −1 Å, the conductance rises exponentially. Starting at $\Delta z \approx -1$ Å, the conductance increases sharply from $\approx 0.03\ G_0$ to $\approx 0.26\ G_0$ over a displacement range $\delta \approx 0.45$ Å. In this regime (II), the transition from tunneling to contact occurs. Although it appears continuous in Figure 2 (owing to low time resolution of data acquisition (≈0.1 ms)), the conductance of the molecular junction is fluctuating rapidly (see below and Figure 2b). Contact is established in regime III, where a bond between the tip apex and the molecule is formed.[12] At contact, the conductance increases slowly upon further tip approach.

Our experiments have been performed repeatedly with different tips on different molecules. Once a sufficiently sharp and stable tip was obtained, essentially identical data sets (neglecting the fluctuations in region II) were recorded hundreds of times as long as the current remained below ≈12 μA. Histograms of the normalized conductance variation, $(G - \langle G \rangle)/\langle G \rangle$, illustrate the reproducibility of the data for the case of a type **1** molecule (Figure 2b). A set of 500 individual conductance curves was averaged giving an arithmetic mean, $\langle G \rangle$, at each tip displacement. In the histogram plotted in Figure 2b the deviations from $\langle G \rangle$ were determined at arbitrarily chosen displacements in the tunneling, transition, and contact regime for each individual conductance trace. Gaussian fits to the statistical data (solid lines) reveal that the fluctuations are most significant in the transition regime.

While conductance curves for all C_{60} orientations exhibit the same general characteristics summarized above, there are important differences in the transition and contact regimes that are specific to a particular orientation (Figure 3). Two

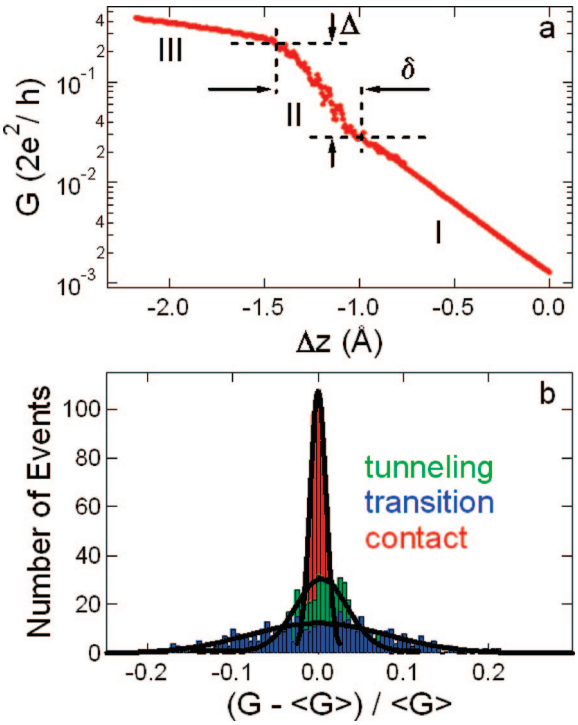

Figure 2. (a) Conductance G of a C_{60} molecule with orientation **1** vs tip displacement Δz. Data are an average over 500 individual conductance traces. Decreasing displacements correspond to closer tip−molecule distances. Tunneling, transition, and contact regimes are indicated by I, II, and III, respectively. $\delta \approx 0.45$ Å and $\Delta \approx 0.23\ G_0$ denote the width of the transition interval and the change of conductance within this interval, respectively. (b) Histograms of deviations from the average conductance $\langle G \rangle$ in the tunneling, transition, and contact regimes from a set of 500 conductance traces. Solid lines depict Gaussian fits.

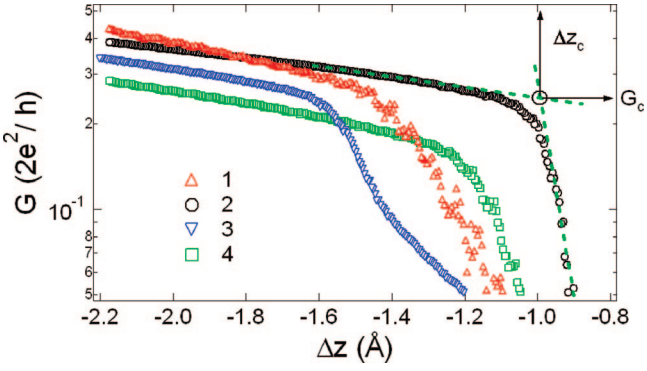

Figure 3. Conductance curves of C_{60} orientations in the transition and contact regimes. Dashed lines are exponential extrapolations of the conductance curves in the tunneling and contact intervals. Their intersections are used for a practical definition of the displacement Δz_c for reaching contact and of the contact conductance G_c. Prior to conductance measurement, the tunneling gap was set at 0.4 V and 1 μA for each curve.

observations are striking: (i) the displacement Δz_c where contact occurs and (ii) the conductance G_c at contact are characteristic of the molecular orientations. For a more quantitative comparison, we extracted Δz_c and G_c as graphically defined in Figure 3 and summarize the results in Table 1.

We first discuss Δz_c, which varies from ≈ -1.0 Å (molecules type **2**) to ≈ -1.6 Å (molecules type **3**). This

Table 1. Comparison of Contact Displacements Δz_c and Conductances G_c for C_{60} Molecules Exhibiting Orientations **1**−**4**

orientation	Δz_c (Å)	G_c (G_0)
1	−1.39	0.26
2	−0.98	0.25
3	−1.57	0.26
4	−1.18	0.17

variation is related to the spatial extension of the lowest unoccupied molecular orbital (LUMO) into vacuum. All conductance curves start at a common conductance determined by the STM feedback parameters used prior to opening the feedback loop. In other words, the displacement $\Delta z = 0$ corresponds to $I = 1$ μA and $V = 0.4$ V. The LUMO extension can be evaluated from constant-current STM images recorded at 0.4 V (not shown), where the LUMO is probed. The apparent height of molecules adsorbed in the same missing row of the Cu(100) substrate differ by ≈ 0.4 Å and thus reflect the differences in Δz_c for molecules **1**, **2** and **3**, **4** (see Table 1). As a consequence, the tip trajectory starts at different heights above the respective molecules and therefore the tip must be displaced over different distances until contact is reached.

Next we address the contact conductance G_c. Molecule type **4**, which exposes a hexagon toward the tip, is significantly less conducting than molecules **1**, **2**, and **3.** Within experimental accuracy, the contact conductance of the latter orientations are rather similar. We have observed identical contact conductances for voltages between 0.05 and 0.6 V. Voltages higher than 0.6 V resulted in less reproducible results. Because 0.6 V corresponds to roughly the energy of the LUMO, enhanced heating of the molecule is likely, which in turn may be responsible for the observed instabilities. Therefore, it was only possible to explore the impact of the LUMO on the conductance, the highest occupied molecular orbital (HOMO), and LUMO + 1 falling out of this voltage range (see below). Currently, no detailed calculations of the conductance of molecules **2**, **3**, and **4** are available. Indeed, modeling the conductance properties of a single molecule contact requires the relaxation of the tip, the molecule, and the substrate structure and thus are computationally extremely costly. However, a preliminary interpretation of the low conductance of molecule **4** is suggested by additional experimental data. Spectra of the differential conductance (dI/dV) of C_{60} (Figure 4a), which were recorded in the tunneling regime and are fairly independent of the C_{60} orientation, show that the LUMO contributes most of the molecular conductance at and below sample voltages of 0.4 V, where the conductance data of Figure 3 were recorded. Differential conductance peaks related to the HOMO and the LUMO + 1 appear at widely different energies of ≈ -1.9 and ≈ 1.8 eV, respectively. We can therefore safely assume that the LUMO contributes considerably to electron transport through the molecule at low bias. Preliminary calculations[26] indicate that the main transport channel of the tip is provided by the 4s orbital of the Cu tip apex atom. A second channel, the 4p orbital, is less conducting by an order of magnitude. We combined the available information and estimated the overlap of the Cu

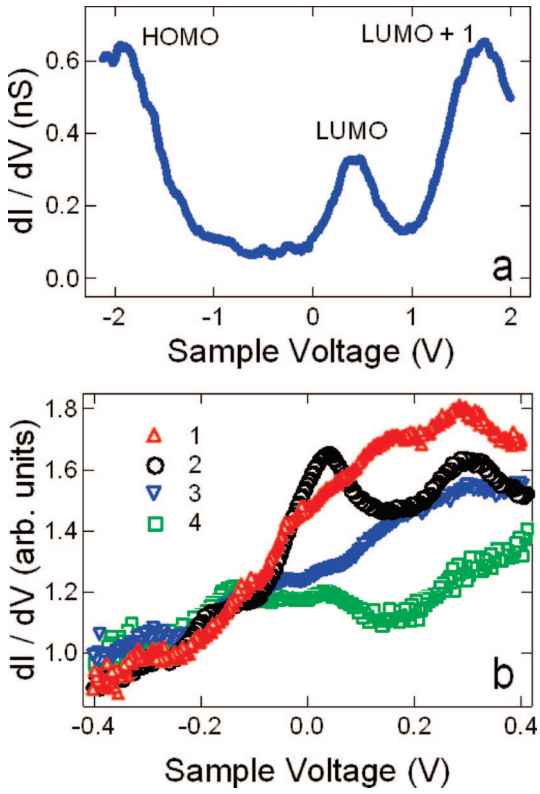

Figure 4. (a) Spectrum of the differential conductance (d*I*/d*V*) acquired on a single C_{60} molecule in the tunneling regime. The spectrum is fairly insensitive to the molecular orientation. Peaks are attributed to the highest occupied molecular orbital (HOMO), the lowest unoccupied molecular orbital (LUMO), and the second-to-lowest molecular orbital (LUMO + 1). Feedback loop was opened at 2 V and 1 nA. (b) d*I*/d*V* spectra at contact for the different molecular orientations. For comparison, spectra were normalized to conductance at −0.4 V.

4s orbital at the tip apex with the C_{60} LUMO for the different orientations by calculating their volume of intersection. The Cu 4s orbital is represented by a sphere with 2.5 Å diameter, which corresponds to the nearest-neighbor distance in a copper crystal. The LUMO is approximated by a torus as reported in ref 25. The 4s orbital is placed at a distance of 5.4 Å from the center of the C_{60} cage as calculated in ref 12. Consistent with the experimentally measured G_c, the overlap of molecule **1** is largest while the overlap of molecule **4** is smallest. While yielding a correct sequence of conductances, the model clearly is too simple for reliable predictions. Nevertheless, it provides further indication of the relevance of conductance through the LUMO at low voltages.

Above, we used tunneling d*I*/d*V* spectra in analyzing contact data. A priori, it is not at all clear that the molecular orbitals remain unchanged at contact, and previous work on metal contacts has revealed Stark shifts of electronic states.[27,28] To address this issue, we recorded spectra of the differential conductance at contact. Somewhat surprisingly, the molecular junctions are sufficiently stable to enable this type of measurement. Results are presented in Figure 4b. While d*I*/d*V* spectra in the tunneling regime vary little even at elevated currents, significantly altered characteristics are observed at contact. For instance, molecules **1** and **3** exhibit a steady increase of their d*I*/d*V* signal, while molecule **2** gives rise to peaks at ≈0.04 V and at ≈0.3 V. Molecule **4** exhibits a slow overall increase of its d*I*/d*V* signal over the explored energy range. From these spectra, we infer that the signature of the LUMO is still present for all molecules, but it is significantly modified depending on the molecular orientation.

The influence of the second electrode, namely the substrate surface, on the molecule conductance also has to be considered. Liang and Ghosh[29] have recently identified contact effects in the electronic conduction through C_{60} adsorbed on Si(100). In good agreement with experimental results,[30,31] they found theoretically that d*I*/d*V* spectra depend on the nature of the molecule−substrate bonding, i.e., the position, the width, as well as the number of peaks depend on the number of covalent bonds, on the adsorption distance, as well as on the character of the bonding (physisorption or chemisorption). In our experiments, spectroscopy of d*I*/d*V* in the tunneling regime on each of the four molecules reveals that the HOMO, the LUMO, and the LUMO + 1 exhibit identical energies and widths for the different orientations. These data suggest that the charge transfer and thus the bonding between the molecules and the substrate are similar. One may speculate that the molecules average over the details of the bonding because several structural elements (carbon pentagons and hexagons) with their specific electronic states are involved in the contact to the reconstructed and corrugated substrate. At contact, the situation is markedly different, and we find that the orientations do affect the conductances. Given that the tips we use are most likely terminated in a single atom, it appears reasonable that the tip side contact to the molecule is more spatially localized and thus more sensitive to the orientation.

In summary, for C_{60} adsorbed on Cu(100), we evidence a molecular orientation that conducts less than others and thus points to the crucial role the electrode−molecule contact geometry plays in conductance measurements. STM-based studies provide a direct relation between junction geometry and conductance data in a single experiment. While currently no detailed model of differential conductance spectra is available for the contact regime, our results suggest a contribution of orbital overlap between tip and molecule to the junction conductance and highlight the changes of the LUMO at contact. We hope that these results will prompt theoretical investigations into a model system that is numerically tractable.

Acknowledgment. We thank Th. Frederiksen and M. Brandbyge (Technical University of Denmark) for discussions and providing results from preliminary calculations. We thank C. Cepek (Laboratorio Nazionale TASC, Italy) for providing clean C_{60} molecules and Ch. Hamann (University of Kiel) for help with figure preparation. Image processing was performed by Nanotec WSxM.[32] We acknowledge financial support by the Deutsche Forschungsgemeinschaft through SFB 677.

References

(1) Reed, M. A.; Lee, T. *Molecular Nanoelectronics*; American Scientific Publishers:: Valencia, CA, 2003.
(2) Flood, A. H.; Stoddart, J. F.; Steuerman, D. W.; Heath, J. R. *Science* **2004**, *306* (5704), 2055.
(3) Hush, N. S. *Ann. N.Y. Acad. Sci.* **2003**, *1006*, 1.
(4) Cuevas, J. C.; Heurich, J.; Pauly, F.; Wenzel, W.; Schön, G. *Nanotechnology* **2003**, *14* (8), 29.
(5) Perebeinos, V.; Tersoff, J.; Avouris, Ph. *Phys. Rev. Lett.* **2005**, *94* (8), 086802.
(6) Reed, M. A.; Zhou, C.; Muller, C. S.; Burgin, T. P.; Tour, J. M. *Science* **1997**, *278* (5336), 252.
(7) Reichert, J.; Ochs, R.; Beckmann, D.; Weber, H. B.; Mayor, M.; v. Löhneysen, H *Phys. Rev. Lett.* **2002**, *88* (17), 176804.
(8) Park, J.; Park, J.; Lim, A. K. L.; Anderson, E: H.; Alivisatos, A. P.; McEuen, P. L. *Nature* **2000**, *407* (6800), 57.
(9) Joachim, C.; Gimzewski, J. K.; Schlittler, R. R.; Chavy, C. *Phys. Rev. Lett.* **1995**, *74* (11), 2102.
(10) Cui, X. D.; Primak, A.; Zarate, X.; Tomfohr, J.; Sankey, O. F.; Moore, A. L.; Moore, T. A.; Gust, D.; Harris, G.; Lindsay, S. M. *Science* **2001**, *294* (5542), 571.
(11) Limot, L.; Kröger, J.; Berndt, R.; Garcia-Lekue, A.; Hofer, W. A. *Phys. Rev. Lett.* **2005**, *94* (12), 126102.
(12) Néel, N.; Kröger, J.; Limot, L.; Frederiksen, T.; Brandbyge, M.; Berndt, R. *Phys. Rev. Lett.* **2007**, *98* (6), 065502.
(13) Kröger, J.; Jensen, H.; Berndt, R. *New J. Phys.* **2007**, *9* (5), 153.
(14) Langlais, V. J.; Schlittler, R. R.; Tang, H.; Gourdon, A.; Joachim, C.; Gimzewski, J. K. *Phys. Rev. Lett.* **1999**, *83* (14), 2809.
(15) Nazin, G. V.; Qiu, X. H.; Ho, W. *Science* **2003**, *302* (5642), 77.
(16) Venkataraman, L.; Klare, J. E.; Nuckolls, C.; Hybertsen, M. S.; Steigerwald, M. L. *Nature* **2006**, *442* (7105), 904.
(17) Böhler, T.; Edtbauer, A.; Scheer, E. *Phys. Rev. B* **2007**, *76* (12), 125432.
(18) Sørensen, M. R.; Brandbyge, M.; Jacobsen, K. W. *Phys. Rev. B* **1998**, *57* (6), 3283.
(19) Xue, Y.; Ratner, M. A. *Phys. Rev. B* **2003**, *68* (11), 115406.
(20) Xue, Y.; Ratner, M. A. *Phys. Rev. B* **2003**, *68* (11), 115407.
(21) Agraït, N.; Levy Yeyati, A.; van Ruitenbeek, J. M. *Phys. Rep.* **2003**, *377* (2−3), 81.
(22) Untiedt, C.; Caturla, M. J.; Calvo, M. R.; Palacios, J. J.; Segers, R. C.; van Ruitenbeek, J. M. *Phys. Rev. Lett.* **2007**, *98* (20), 206801.
(23) Abel, M.; Dmitriev, A.; Fasel, R.; Liu, N.; Barth, J. V.; Kern, K. *Phys. Rev. B* **2003**, *67* (24), 245407.
(24) Hou, J. G.; Jinlong, Y.; Haiqian, W.; Qunxiang, L.; Changgan, Z.; Hai, L.; Wang, B.; Chen, D. M.; Qingshi, Z. *Phys. Rev. Lett.* **1999**, *83* (15), 3001.
(25) Lu, X.; Grobis, M.; Khoo, K. H.; Crommie, M. F.; Louie, S. G. *Phys. Rev. Lett.* **2003**, *90* (9), 096802.
(26) Frederiksen, T.; Brandbyge, M. Private communication.
(27) Limot, L.; Maroutian, T.; Johansson, P.; Berndt, R. *Phys. Rev. Lett.* **2003**, *91* (19), 196801.
(28) Kröger, J.; Limot, L.; Jensen, H.; Berndt, R.; Johansson, P. *Phys. Rev. B* **2004**, *70* (3), 033401.
(29) Liang, G.-C.; Ghosh, A. W. *Phys. Rev. Lett.* **2005**, *95* (7), 076403.
(30) Yao, X.; Ruskell, T. G.; Workman, R. K.; Sarid, D.; Chen, D. *Surf. Sci.* **1996**, *366* (3), L743.
(31) Dunn, A. W.; Svensson, E. D.; Dekker, C. *Surf. Sci.* **2002**, *498* (3), 237.
(32) Horcas, I.; Fernández, R.; Gómez-Rodríguez, J. M.; Colchero, J.; Gómez-Herrero, J.; Baro, A. M. *Rev. Sci. Instrum.* **2007**, *78* (1), 013705.

NL073074I